Electromagnetic Scattering from Two Adjacent Objects

Kamal Sarabandi, *Senior Member, IEEE*, and Paul F. Polatin

Abstract—**In this paper, the problem of electromagnetic scattering from two adjacent particles is considered and an iterative solution that accounts for multiple scattering up to second-order is proposed. The first-order solution can easily be obtained by calculating the scattered field of isolated particles when illuminated by a plane-wave. To get the second-order solution, the scattered field from one of the particles, with nonuniform phase, amplitude, and polarization, is considered as the illuminating wave for the other particle and vice versa. In this work, the second-order scattered field is derived analytically using a novel technique based on the reciprocity theorem. In specific, the analytical solution for bistatic specular scattering from a cylinder and sphere pair is discussed and the results are compared with numerical computations based on the method of moments.**

I. Introduction

THE study of discrete random media has important application in the understanding of remotely sensed data. In particular, the interaction of electromagnetic waves with forest stands and other types of vegetation cover is of interest because of the important role such vegetation plays in the regulation of environmental and climatic change. Typical canopies consist of objects such as trunks, stems, branches and leaves or needles and, in general, vegetation tends to have some complex structural features. However, analytical solutions for the problem of scattering of electromagnetic plane-waves by objects exist for only a limited number of canonical geometries. If the scattering body is inhomogeneous, or the polarization and phase front of the illuminating field is nonuniform, analytical solutions of the vector wave equation do not exist even for canonical geometries.

Almost all models that are currently being used for the analysis of EM scattering from collections of discrete scatterers rely on the single scattering properties of the constituent particles [1]–[4]. However, when the sizes and/or number densities of the scatterers become large enough that they are in the near-field of each other, solutions based on their single scattering properties are no longer valid. Certain types of vegetation canopies such as forest stands and some agricultural fields have high number densities of strong scatterers [5]–[7]. In addition, the particle sizes in these canopies are large enough so that adjacent scatterers are not in each others far-field zone, especially in the microwave region.

Manuscript received May 13, 1993; revised November 15, 1993.

K. Sarabandi is with the Department of Electrical Engineering and Computer Science, The University of Michigan, Ann Arbor, MI 48109-2122.

P. F. Polatin is with the MITRE Corporation, Bedford, MA.

IEEE Log Number 9400496.

To model vegetation of this type, it is necessary to be able to treat electromagnetic interactions between particles that are not only nonplane-wave in character but have nonuniformities in amplitude, phase, and polarization. As has been stated, it is impossible to find exact analytical solutions for this type of problem except in a small number of cases [8], [9]. In some few circumstances it may be possible to obtain an analytical solution by employing a plane-wave expansion technique [10] or some other specialized approach. Even so, such solutions may yield results that are difficult to evaluate or have tedious multiple integrations that must be done numerically. This is obviously a distinct disadvantage when the desired end result is to simulate EM scattering from a dense random medium.

EM modeling of vegetation canopies usually involves the construction of simplified geometrical representations for the constituent scattering elements [11]–[14]. When this is the case, it is a fairly simple matter to obtain expressions for the first-order scattered field using the single-scattering properties of the isolated particles when the primary excitation is a plane-wave. To obtain the secondary scattered field from interacting particles it is necessary to account for illumination of the secondary scatterer by the scattered field from the primary scatterer. This paper presents a technique for obtaining the secondary scattered field analytically by employing the reciprocity theorem. The technique is then applied to obtain an analytical solution for bistatic scattering from a cylinder-sphere pair. This cylinder-sphere interaction has some importance because, along with the electromagnetic coupling between pairs of cylinders, it provides a basic building block from which the EM scattering properties of a heterogeneous two-component forest canopy may be simulated. The results of analytical field calculations for cylinder-sphere pairs are then compared with numerical computations based on the method of moments.

II. Secondary Scattered Field from Reciprocity

In this section, a procedure utilizing reciprocity for evaluation of the secondary scattered field from a particle when illuminated by the primary scattered field of another adjacent particle is outlined. The reciprocity theorem simplifies this evaluation significantly when the observation point is in the far-field zone of both particles. Derivation of the expression for the secondary scattered field of perfectly conducting particles is slightly different from that of dielectric particles. First we consider perfectly conducting particles. Suppose the incident field induces a surface current density $\boldsymbol{J}_1$ on the surface of particle #1 in absence of particle #2. The objective is evaluation of the scattered field from particle #2 with $\boldsymbol{J}_1$ as

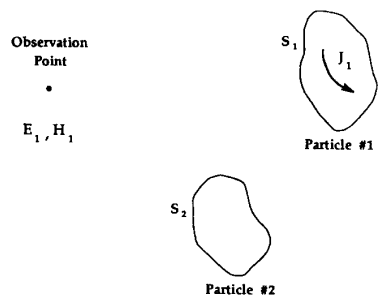

Fig. 1. Induced current on particle #1 produces scattered field from particle #2.

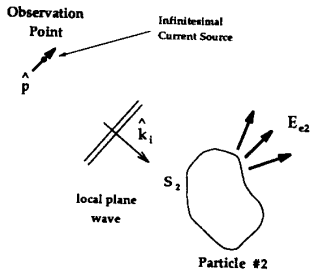

Fig. 2. Particle #1 removed and elementary current source placed at observation point.

the excitation source. Suppose the electric and magnetic fields produced by $\boldsymbol{J}_1$ (as an impressed source) in the presence of particle #2 are denoted by $\boldsymbol{E}_1$ and $\boldsymbol{H}_1$, respectively, as shown in Fig. 1. Obviously $\boldsymbol{E}_1$ and $\boldsymbol{H}_1$ satisfy Maxwell's equations everywhere in the medium.

Now, let us consider another situation where the source $\boldsymbol{J}_1$ is removed and an infinitesimal current source $\boldsymbol{J}_e$ given by

$$\boldsymbol{J}_e = \hat{p}\delta(\boldsymbol{r} - \boldsymbol{r}_p)$$

is placed at observation point P as in Fig. 2. The electric and magnetic fields produced by the elementary current source are denoted by $\boldsymbol{E}_{e2}$ and $\boldsymbol{H}_{e2}$ and also satisfy Maxwell's equations. Applying the reaction theorem [15] to fields $\boldsymbol{E}_1$, $\boldsymbol{E}_{e2}$, $\boldsymbol{H}_1$, and $\boldsymbol{H}_{e2}$ over the entire medium, it can be shown that

$$\int_{S_2+S_\infty} (\boldsymbol{E}_1 \times \boldsymbol{H}_{e2} - \boldsymbol{E}_{e2} \times \boldsymbol{H}_1) \cdot \hat{n}\, ds = -\int_{S_1} \boldsymbol{J}_1 \cdot \boldsymbol{E}_{e2}\, ds + \hat{p} \cdot E_1 \quad (1)$$

where S_∞ represents a closed sphere at infinity. Since at distant points $\boldsymbol{E}_j = Z_0 \boldsymbol{H}_j \times \hat{n}$, where $j = 1, e2$, the surface integral over S_∞ vanishes. Also the surface integral over the surface of particle #2 vanishes since $\hat{n} \times \boldsymbol{E} = 0$ over a perfectly conducting surface.

Since the elementary current source $\boldsymbol{J}_e$ is in the far-field zone of particle #2, $\boldsymbol{E}_{e2}$ can be approximated by the sum the scattered field of particle #2 when illuminated by a plane-wave and the direct field generated by the elementary source itself. Noting that $\boldsymbol{J}_1$ is a function of the incident wave polarization $(\hat{v}_i, \hat{h}_i)$ and the polarization of the elementary source $\hat{p}$ can also be chosen to be either $\hat{v}$ or $\hat{h}_s$, the expression for the scattered field is given by

$$\hat{p} \cdot \boldsymbol{E}_1^s = \int_{S_1} \boldsymbol{E}_{e2}(\hat{v}_s, \hat{h}_s) \cdot \boldsymbol{J}_1(\hat{v}_i, \hat{h}_i)\, ds \quad (2)$$

where $(\hat{v}_i, \hat{h}_i)$ and $(\hat{v}_s, \hat{h}_s)$ are sets of perpendicular unit vectors normal to the incidence and scattering directions, respectively. The scattered field from particle #1 when illuminated by the field generated from the induced current on particle #2 can be obtained in a similar manner and is given by

$$\hat{p} \cdot \boldsymbol{E}_2^s = \int_{S_2} \boldsymbol{E}_{e1}(\hat{v}_s, \hat{h}_s) \cdot \boldsymbol{J}_2(\hat{v}_i, \hat{h}_i)\, ds. \quad (3)$$

Here, $\boldsymbol{E}_{e1}(\hat{v}_s, \hat{h}_s)$ is the sum of the radiated field from the elementary current source and the scattered field of particle #1 when illuminated by this elementary source. The source is characterized as possessing either a vertical or a horizontal polarization state and is located at the point of observation. It should be noted that $\boldsymbol{E}_1^s$ includes the first-order scattered field of particle #1 and secondary scattered field of particle #2. Identically, $\boldsymbol{E}_2^s$ includes the first-order scattered field of particle #2 plus the secondary scattered field of particle #1. Therefore $\boldsymbol{E}_1^s + \boldsymbol{E}_2^s$ is the total scattered field of both particles up to second-order.

Now let us consider the case in which both particles are dielectric objects. The incident wave induces a polarization current $\boldsymbol{J}_1$ in particle #1 in the absence of particle #2. When particle #2 is placed at its location with no incident wave present, the volumetric current $\boldsymbol{J}_1$ induces a volumetric current $\boldsymbol{J}_{12}$ in particle #2. The total fields in this case will be denoted by $\boldsymbol{E}_1$ and $\boldsymbol{H}_1$. In a second experiment, we place the elementary current source $\boldsymbol{J}_e$ at the observation point as before and remove the current source $\boldsymbol{J}_1$ (particle #1). The elementary current then induces a volumetric current $\boldsymbol{J}_{e2}$ in particle #2 for which the electric and magnetic fields will be denoted as $\boldsymbol{E}_{e2}$ and $\boldsymbol{H}_{e2}$. The currents induced in particle #2 may be expressed in terms of the total electric field and relative dielectric constant (ϵ_2) of particle #2. They are given by

$$\boldsymbol{J}_{12}(\boldsymbol{r}) = -ik_0 Y_0(\epsilon_2 - 1)\boldsymbol{E}_1(r), \qquad r \in V_2 \quad (4)$$

$$\boldsymbol{J}_{e2}(\boldsymbol{r}) = -ik_0 Y_0(\epsilon_2 - 1)\boldsymbol{E}_{e2}(r), \qquad r \in V_2 \quad (5)$$

where k_0 and Y_0 are the wave number and characteristic admittance of free space, respectively, and V_2 is the region occupied by particle #2. Application of the reaction theorem over the entire medium results in

$$\int_{S_\infty} (\boldsymbol{E}_1 \times \boldsymbol{H}_{e2} - \boldsymbol{E}_{e2} \times \boldsymbol{H}_1) \cdot \hat{n}\, ds = -\int_{V_1} \boldsymbol{J}_1 \cdot \boldsymbol{E}_{e2}\, dv - \int_{V_2} \boldsymbol{J}_{12} \cdot \boldsymbol{E}_{e2}\, dv + \int_{V_2} \boldsymbol{J}_{2e} \cdot \boldsymbol{E}_1\, dv + \hat{p} \cdot \boldsymbol{E}_1.$$

The integral on the left-hand side vanishes as before, and, by substituting (4) and (5) into the second and third integrals on the right-hand side, it can be shown that the last two integrals in the expression given above cancel each other. Thus, the

sum of the primary scattered field of particle #1 and the second-order scattered field of particle #2 is given by

$$\hat{p} \cdot \boldsymbol{E}_1 = \int_{V_1} \boldsymbol{J}_1 \cdot \boldsymbol{E}_{e2}\, dv. \tag{6}$$

Similarly, the sum of the scattered field of particle #2 and the second-order scattered field of particle #1 is given by

$$\hat{p} \cdot \boldsymbol{E}_2 = \int_{V_2} \boldsymbol{J}_2 \cdot \boldsymbol{E}_{e1}\, dv. \tag{7}$$

In (7), $\boldsymbol{J}_2$ is the volumetric current induced in particle #2 by the incident wave in the absence of particle #1 and $\boldsymbol{E}_{e1}$ is the total field of the elementary current located at the observation point in the presence of particle #1.

When one of the particles is dielectric and the other one is metallic, the expressions for the scattered fields can be obtained in a similar way. Let us say that particle #1 is metallic and particle #2 dielectric, then the expressions for the scattered fields are given by (2) and (7), respectively. Conversely, if particle #1 is dielectric and particle #2 metallic, expressions (6) and (3) give the scattered fields.

III. Electromagnetic Scattering from a Cylinder-Sphere Pair

The expressions for the scattered fields from the two particles as derived in the previous section are very general and can be applied to any particle pair with known geometries and dielectric properties. In this calculation only the scattered fields and induced currents of isolated particles when illuminated by a plane-wave are required. The sphere and cylinder are among the few geometries for which an exact analytical scattering solution is known. Additionally, as mentioned previously, a collection of randomly positioned spheres and vertical cylinders above a ground plane can be used to simulate a heterogeneous forest medium which includes the effect of multiple scattering between canopy components.

Analytical evaluation of the integrals (2), (3), (6), and (7), even for the cylinder-sphere pair, is not possible, and one must resort to numerical methods. In this section an approximate analytical solution will be derived for a cylinder-sphere pair. The assumption is made that the cylinder is in the far-field region of the sphere. However, the sphere is assumed to be in the near-field of the cylinder with respect to the cylinder's longitudinal dimension and in the far-field region of the cylinder's transverse dimension. If the radius of the cylinder and sphere are denoted by a_c and a_s, respectively, and the cylinder length is represented by L, then the conditions previously specified may be stated mathematically as

$$\tilde{\rho} > \frac{2a_s^2}{\lambda}, \quad \frac{L^2}{\lambda} \geq \tilde{\rho} > \frac{2a_c^2}{\lambda} \tag{8}$$

where $\tilde{\rho}$ is the distance between the cylinder axis and the sphere center.

Suppose a plane-wave, whose direction of propagation is denoted by $\hat{k}_i$, is incident on a cylinder-sphere pair and is given by

$$\boldsymbol{E}_i = \hat{e}_i e^{ik_0 \hat{k}_i \cdot \mathbf{r}}.$$

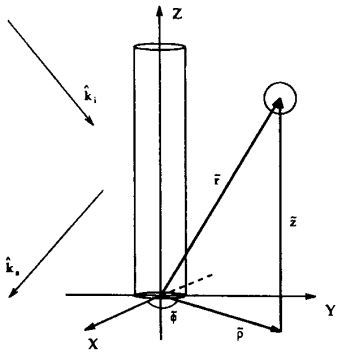

Fig. 3. Geometry and coordinates of the cylinder/sphere pair.

The cylinder axis coincides with the z-axis of the Cartesian coordinate system and the sphere center is located at $\tilde{\boldsymbol{r}} = \tilde{\rho}\cos\tilde{\phi}\hat{x} + \tilde{\rho}\sin\tilde{\phi}\hat{y} + \tilde{z}\hat{z}$. The observation point is located at a distance r_0 in the direction $\hat{k}_s$. The geometry of the problem is given in Fig. 3.

The current induced on the sphere when illuminated by a plane-wave can be easily computed by the standard method of separation of variables [16]. Since the cylinder is assumed to be much longer than the excitation wavelength, the current induced in this finite length cylinder can be approximated by that in an infinitely long cylinder of the same radius and electrical properties [17], [18]. The field generated by the elementary current source located at the observation point, over the volume (surface) of each scatterer when the other one is absent is calculated as follows. Let us first consider the case where the sphere is absent. The field generated by the elementary current $\boldsymbol{J}_e = \hat{p}\delta(\boldsymbol{r} - \boldsymbol{r}_o)$ is composed of two components. The first component is the direct contribution of the current source and is given in the far zone by

$$\boldsymbol{E}_{ed}(r) = \frac{-ik_0 Z_0}{4\pi r_0} e^{ik_0 r_0} e^{-ik_0 \hat{k}_s \cdot r} \hat{k}_s \times \hat{k}_s \times \hat{p}. \tag{9}$$

The second component is the scattered field from the cylinder when illuminated by the radiated field of the elementary current source. This illuminating field can be approximated locally by a plane-wave propagating along the $-\hat{k}_s$ direction. Since the point $\boldsymbol{r}$ is in the near-field of the cylinder which satisfies condition (8), the scattered field is given by [10]

$$\boldsymbol{E}_{ec}(\boldsymbol{r}) = \frac{-ik_0 Z_0 e^{ik_0 r_0}}{4\pi r_0} \boldsymbol{F}(\phi - \phi_s) \cdot H_0^{(1)}(k_0 \sin\theta_s \rho) e^{-ik_0 \cos\theta_s z} \tag{10}$$

where (ρ, ϕ, z) is the cylindrical coordinate of position vector $\boldsymbol{r}$, $H_0^{(1)}$ is the Hankel function of the first kind and zeroth order, and θ_s and ϕ_s are the spherical angles specifying the unit vector $\hat{k}_s$, that is

$$\hat{k}_s = \sin\theta_s \cos\phi_s \hat{x} + \sin\theta_s \sin\phi_s \hat{y} + \cos\theta_s \hat{z}. \tag{11}$$

The expression for the vector quantity $\boldsymbol{F}(\phi - \phi_s)$ in (10) is given by

$$\boldsymbol{F}(\phi - \phi_s) = \frac{-1}{\sin^2\theta_s} \sum_{m=-\infty}^{+\infty} (-1)^m \cdot [A_m^s(\hat{k}' \times \hat{k}' \times \hat{z}) + B_m^s(\hat{k}' \times \hat{z})] e^{im(\phi - \phi_s)}$$

where

$$\hat{k}' = \sin\theta_s[\cos\phi\hat{x} + \sin\phi\hat{y}] - \cos\theta_s\hat{z}$$

and

$$A_m^s = C_m^{TM}\hat{k}_s \times (\hat{k}_s \times \hat{p}) \cdot \hat{z} + i\overline{C}_m(\hat{k}_s \times \hat{p}) \cdot \hat{z}$$

$$B_m^s = C_m^{TE}(\hat{k}_s \times \hat{p}) \cdot \hat{z} - i\overline{C}_m\hat{k}_s \times (\hat{k}_s \times \hat{p}) \cdot \hat{z}.$$

The expressions for C_m^{TM}, C_m^{TE}, and $\overline{C}_m$ are given in [19].

The direct scattered field from the sphere and the secondary scattered field from the cylinder can be obtained from (2) or (6) depending on whether the sphere is perfectly conducting or dielectric. The first component of this scattered field is due to the excitation $\boldsymbol{E}_{ed}(\boldsymbol{r})$ which yields the direct contribution from the sphere. This is specified by

$$\hat{p} \cdot \boldsymbol{E}_{1s} = \int_{\text{sph.}} \boldsymbol{J}_s(\boldsymbol{r}) \cdot \boldsymbol{E}_{ed}(\boldsymbol{r})\, dv.$$

Using the far-field expression for $\boldsymbol{E}_{ed}(\boldsymbol{r})$, it can be shown that

$$\begin{aligned}\hat{p} \cdot \boldsymbol{E}_{1s} &= \frac{e^{ik_0 r_0}}{r_0}(-k_0^2) \cdot \left[\hat{k}_s \times \left(\hat{k}_s \times \frac{iZ_0}{4\pi k_0}\int \boldsymbol{J}_s(\boldsymbol{r}) e^{-ik_0\hat{k}_s\cdot\boldsymbol{r}}\, dv\right)\right] \cdot \hat{p} \\ &= \frac{e^{ik_0 r_0}}{r_0} e^{ik_0(\hat{k}_i - \hat{k}_s)\cdot\tilde{r}} \boldsymbol{S}_s(\hat{k}_i, \hat{k}_s) \cdot \hat{p} \qquad (12)\end{aligned}$$

where $\boldsymbol{S}_s(\hat{k}_i, \hat{k}_s)$ is the bistatic scattering amplitude of the isolated sphere.

The second component of the scattered field is referred to here as the sphere-cylinder interaction and is given by

$$\hat{p} \cdot \boldsymbol{E}_{1sc} = \int_{\text{sph.}} \boldsymbol{J}_s(r) \cdot \boldsymbol{E}_{ec}(\boldsymbol{r})\, dv. \qquad (13)$$

Integral (13) can be evaluated analytically, keeping in mind the conditions on the dimensions of, and distance between, the particles as specified in (8). Under these conditions the angle subtended by the sphere is small, therefore $\boldsymbol{F}(\phi - \phi_s) \simeq \boldsymbol{F}(\tilde{\phi} - \phi_s)$ which is a constant vector and comes out of the integral. Also the Hankel function can be approximated by

$$\begin{aligned}&H_0^{(1)}(k_0 \sin\theta_s\rho) e^{-ik_0\cos\theta_s z} \\ &\qquad \simeq H_0^{(1)}(k_0 \sin\theta_s\tilde{\rho}) e^{-ik_0\cos\theta_s\tilde{z}} \exp[-ik_0\hat{\tilde{k}} \cdot r']\end{aligned}$$

noting that ρ and $\hat{\rho}$ can be approximated by $\tilde{\rho}$ and $\hat{\tilde{\rho}}$, respectively. Here, $\hat{\tilde{k}} = -\sin\theta_s\hat{\tilde{\rho}} + \cos\theta_s\hat{z}$ and $\boldsymbol{r}' = \boldsymbol{r} - \tilde{\boldsymbol{r}}$

Thus, the sphere-cylinder interaction term is obtained from

$$\begin{aligned}\hat{p} \cdot \boldsymbol{E}_{1sc} = \frac{-1}{\sin^2\theta_s}\frac{e^{ik_0 r_0}}{r_0} H_0^{(1)}(k_0 \sin\theta_s\tilde{\rho}) e^{-ik_0\cos\theta_s\tilde{z}} \\ \cdot \left\{\left[\sum_{m=-\infty}^{+\infty} A_m^s e^{im(\tilde{\phi} - \phi_s)}\right] \boldsymbol{E}_s^s\left(\hat{k}_i, \hat{\tilde{k}}\right) \cdot \hat{z} \right. \\ \left. + \left[\sum_{m=-\infty}^{+\infty} B_m^s e^{im(\tilde{\phi} - \phi_s)}\right] \left(\hat{\tilde{k}} \times \boldsymbol{E}_s^s(\hat{k}_i, \hat{\tilde{k}})\right) \cdot \hat{z}\right\}\end{aligned}$$

where $\boldsymbol{E}_s^s(\hat{k}_i, \hat{\tilde{k}})$ is the bistatic scattered field amplitude of the isolated sphere.

Now we consider the case for which the cylinder is absent and evaluate the field generated by the elementary current source. As previously, the total field generated by the elementary current consists of two components. The first component is the direct field given by (9), and the second component is the scattered field from the sphere when illuminated by the direct field of the elementary current source. Noting that this current source is in the far-field of the cylinder-sphere pair, the sphere illumination appears locally as a plane-wave. Since the cylinder is in the far-field of the sphere, the second component, in the vicinity of the cylinder axis, is given by

$$\boldsymbol{E}_{es}(\boldsymbol{r}) = \frac{-ik_0 Z_0}{4\pi}\frac{e^{ik_0 r_0}}{r_0} e^{-ik_0\hat{k}_s\cdot\tilde{\boldsymbol{r}}} \cdot \frac{e^{ik_0 r'}}{r'} \boldsymbol{S}_s(-\hat{k}_s, \hat{r}')$$

where r' is the distance between the sphere center and the point at $\boldsymbol{r}$, that is $r' = |\boldsymbol{r} - \tilde{\boldsymbol{r}}|$ and $\hat{r}' = (\boldsymbol{r} - \tilde{\boldsymbol{r}})/|\boldsymbol{r} - \tilde{\boldsymbol{r}}|$.

The direct scattered field from the cylinder and the secondary scattered field from the sphere can be obtained from (3) or (7) depending on whether the cylinder is perfectly conducting or dielectric. The first component of this field is the direct contribution from the cylinder alone and is given by

$$\hat{p} \cdot \boldsymbol{E}_{2c} = \int_{\text{cyl.}} \boldsymbol{J}_c(r) \cdot \boldsymbol{E}_{ed}(\boldsymbol{r})\, \boldsymbol{dv}.$$

As in (12) it can easily be shown that

$$\hat{p} \cdot \boldsymbol{E}_{2c} = \frac{e^{ik_0 r_0}}{r_0} \boldsymbol{S}_c(\hat{k}_i, \hat{k}_s) \cdot \hat{p} \qquad (14)$$

where $\boldsymbol{S}_c(\hat{k}_i, \hat{k}_s)$ is the far field amplitude of the isolated cylinder given in [20, p. 97].

For analytical evaluation of the cylinder-sphere interaction, it is noted that the current induced in the cylinder has a progressive phase factor along the cylinder axis, that is

$$\boldsymbol{J}_c(\boldsymbol{r}) = \boldsymbol{j}(\rho, \phi) e^{ik_0\cos\theta_i z}.$$

The second term in (7) is given by

$$\begin{aligned}\hat{p} \cdot \boldsymbol{E}_{2cs} = \frac{-ik_0 Z_0}{4\pi}\frac{e^{ik_0 r_0}}{r_0} e^{-ik_0\hat{k}_s\cdot\tilde{r}} \\ \int_s\int_0^L \boldsymbol{j}(\phi, \rho) e^{ik_0\cos\theta_i z} \cdot \boldsymbol{S}_s(-\hat{k}_s, \hat{r}')\frac{e^{ik_0|r - \tilde{r}|}}{|r - \tilde{r}|}\, dz\, ds \qquad (15)\end{aligned}$$

where the first integral is over the cylinder cross-section. By rewriting $|\boldsymbol{r} - \tilde{\boldsymbol{r}}|$ in cylindrical coordinates, i.e., $|\boldsymbol{r} - \tilde{\boldsymbol{r}}| = \sqrt{|\vec{\rho} - \vec{\tilde{\rho}}|^2 + (z - \tilde{z})^2}$ and noting that $k_o|\vec{\rho} - \vec{\tilde{\rho}}| \gg 1$, the

stationary phase approximation can be used to evaluate the z integration. The stationary point of the integrand is at $Z_s = \tilde{z} - \cos\theta_i|\rho - \tilde{\rho}|$ and (15) simplifies to

$$\hat{p}\cdot\boldsymbol{E}_{2cs} = \frac{-ik_0Z_0}{4\pi}\frac{e^{ik_0r_0}}{r_0}e^{-k_0\hat{k}_s\cdot\vec{r}}\int_s H_0^{(1)}(k_0\sin\theta_i|\vec{\rho}-\vec{\tilde{\rho}}|) \cdot j(\rho,\phi)\cdot\boldsymbol{S}_s(-\hat{k}_s,\hat{r}_s')\,\rho d\rho d\phi \quad (16)$$

where $\hat{r}_s'$ is the unit vector $\hat{r}'$ evaluated at the stationary point. Noting that $|\vec{\rho}| \ll |\vec{\tilde{\rho}}|$

$$\hat{r}_s' = -\sin\theta_i\frac{\vec{\rho}-\hat{\tilde{\rho}}}{|\vec{\rho}-\vec{\tilde{\rho}}|} - \cos\theta_i\hat{z} \simeq -\sin\theta_i\hat{\tilde{\rho}} - \cos\theta_i\hat{z}.$$

Under this approximation $\boldsymbol{S}_s(-\hat{k}_s,\hat{r}_s')$ is not a function of the integration variables. Therefore (16) can be written as

$$\hat{p}\cdot\boldsymbol{E}_{2cs} = \frac{-ik_0Z_0}{4\pi}\frac{e^{ik_0r_0}}{r_0}e^{-ik_0\hat{k}_s\cdot\vec{r}}\cdot H_0^{(1)}(k_0\sin\theta_i\tilde{\rho}) \cdot\boldsymbol{S}_s(-\hat{k}_s,\hat{r}_s')\cdot\int_s j(\rho,\phi)e^{-ik_0\sin\theta_i\hat{\tilde{\rho}}\cdot\vec{\rho}}\,\rho d\rho d\phi$$

Note that with values of z for which $Z_s > L$ or $Z_s < 0$ (stationary point outside the cylinder surface) the scattered field $\boldsymbol{E}_{2cs}$ is negligible and can be ignored. The integral in this expression is proportional to the bistatic scattered field amplitude ($\boldsymbol{E}_c^s(\hat{k}_i,-\hat{r}_s')$) of an infinitely long cylinder with the same radius and dielectric constant as those of the finite cylinder. Therefore

$$\hat{p}\cdot\boldsymbol{E}_{2cs} = \frac{i}{\pi}\frac{e^{ik_0r_0}}{r_0}e^{-ik_0\hat{k}_s\cdot\vec{r}} \cdot H_0^{(1)}(k_0\sin\theta_i\tilde{\rho})\boldsymbol{S}_s(-\hat{k}_s,\hat{r}_s')\cdot\boldsymbol{E}_c^s(\hat{k}_i,-\hat{r}_s')$$

where

$$\boldsymbol{E}_c^s(\hat{k}_i,-\hat{r}_s') = \frac{1}{\sin\theta_i}\sum_{m=-\infty}^{+\infty} \cdot[A_m^i(-\cos\theta_i\hat{\tilde{\rho}}+\sin\theta_i\hat{z}) + B_m^i\hat{\tilde{\phi}}]e^{im(\phi_s-\phi_i)}$$

with $\hat{\tilde{\phi}} = \hat{z}\times\hat{\tilde{\rho}}$. and A_m^i and B_m^i given in [20].

The derivation of the scattered field for a cylinder-sphere pair can be easily generalized to a cylinder and an arbitrary scatterer so long as the expression for the scattered field of the isolated scatterer is known and the dimensions of the scatterer satisfy the conditions specified earlier.

IV. Numerical Results

The theoretical development presented in the previous section for second-order scattering from the cylinder-sphere pair has been validated using the Numerical Electromagnetics Code (NEC) [21] which is a computational package based on the method of moments. This approach was chosen because we were interested in the bistatic scattering behavior of the pair, particularly in the forward specular cone, which is quite difficult to obtain experimentally. The forward specular cone is referred to as the set of azimuthal angles for which the scattered wave-vector lies on the conical surface of revolution generated by rotating the incident wave-vector around the z-axis as shown in Fig. 4. This subdomain of the scattering pattern is paticularly important for simulating the interaction of electromagnetic waves with vertical structures above smooth surfaces. In this case, the radar return is dominated by the scattered field in the specular cone.

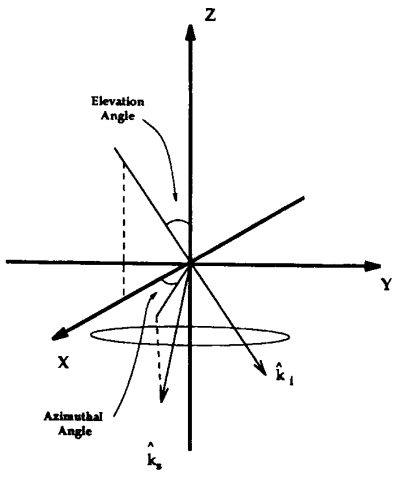

Fig. 4. Scattering geometry and angles for forward specular cone scattering.

The validation for the VV and VH polarization states were made with a model consisting of a cylinder 18.0 cm in length and 0.1 cm in diameter with a finite conductivity of 100 mhos/m, and a perfectly conducting sphere with ka = 1.69 at an excitation frequency of 9.25 GHz. The cylinder was chosen to be of finite conductivity because this damps the axial standing wave pattern that exists on a finite length perfectly conducting cylinder. Our finite length cylinder model does not need to account for this standing wave behavior because in all real vegetation, cylindrical structures are composed of lossy dielectric material and do not support standing waves of significant amplitude. A cylinder having a small diameter as compared with the excitation wavelength was used because the version of NEC we have only provides for finite conductivity in thin wire structures. The number of unknowns for the thin cylinders was on the order of 10 per wavelength or a total of about 60 for the 18 cm length.

The sphere was composed of variable segmented perfectly conducting rectangular patches as described in [22]. A total of 90 rectangular patches were used to represent the sphere. In general, the relative configurations of the cylinder-sphere pair and the scattering patterns were chosen so as to present as great a contrast as possible between the first- and second-order scattering behaviors. The angle of elevation and the azimuthal angle are defined in Fig. 4. The plane of incidence in the x–z plane and the azimuthal incidence angle is 180 degrees. The cylinder is always located at the origin and the relative cylindrical coordinates of the sphere are presented.

Fig. 5 is a VV polarized azimuthal pattern for which the elevation angle is 37 degrees. The relative cylindrical coordinates of the sphere are $(\tilde{\rho},\tilde{\phi},\tilde{z}) = (18\text{ cm}, 180°, 9\text{ cm})$. In this case the cylinder and sphere are located far enough apart to be effectively isolated. This figure demonstrates that the single scattering models for the sphere and cylinder are in

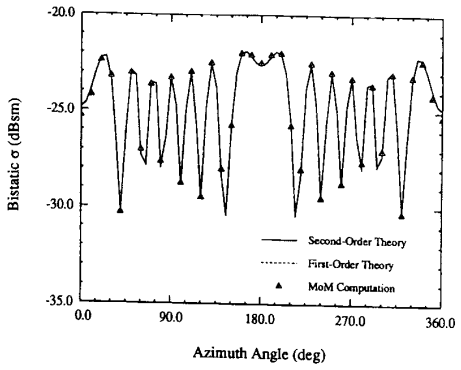

Fig. 5. Cylinder and sphere VV polarized scattering cross section at 9.25 GHz.

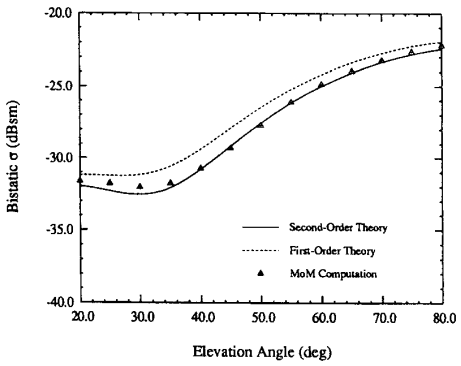

Fig. 7. Cylinder and sphere VV polarized scattering cross section at 9.25 GHz.

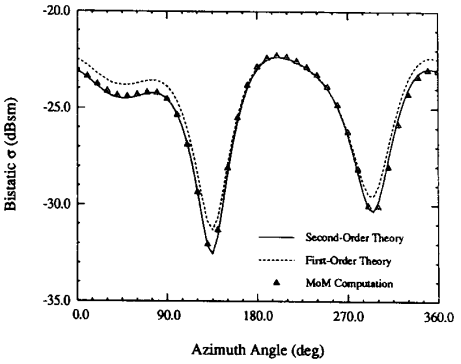

Fig. 6. Cylinder and sphere VV polarized scattering cross section at 9.25 GHz.

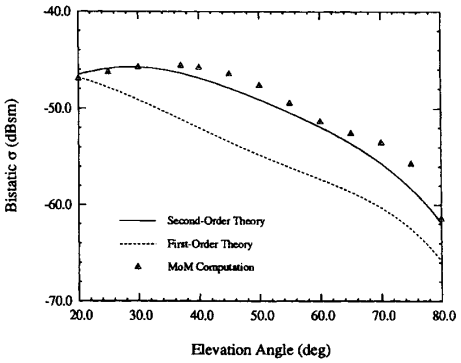

Fig. 8. Cylinder and sphere VH polarized scattering cross section at 9.25 GHz.

agreement with the moment method computation to within less than about 0.2 dB and establishes a baseline for comparison. The oscillatory behavior of the RCS in this figure is simply the interference pattern of the two scattering sources. Figs. 6 and 7 illustrate the VV scattering behavior for the case where the sphere is close to the cylinder. In Fig. 6 the relative cylindrical coordinates of the sphere are $(\tilde{\rho}, \tilde{\phi}, \tilde{z}) = (2\text{ cm}, 45°, 9\text{ cm})$, while in Fig. 7 they are $(\overline{\rho}, \tilde{\phi}, \tilde{z}) = (2.5\text{ cm}, 45°, 9\text{ cm})$. It may be seen from these two figures that the VV second-order result provides a reasonable approximation and is in agreement with the moments method data to within about 0.4 dB over the angular range.

The maximum difference between the first- and second-order cross-polarized (VH) response occurs in regions close to 0 and 180 degrees in azimuthal angle. At these two points the first-order cross-polarized response disappears while the second-order response is low but nonzero. Fig. 8 illustrates the difference between the first- and second-order scattering behavior for the case having relative cylindrical coordinates of $(\overline{\rho}, \tilde{\phi}, \tilde{z}) = (2\text{ cm}, 45°, 9\text{ cm})$ and an azimuthal scattering angle of 350 degrees. This provides good contrast between the scattering orders, and the scattering amplitude is strong enough that the accuracy of the numerical computation is sufficient for comparison. The agreement of the second-order analytical result with the moment method computation has a mean deviation of about 1 dB or so over most of the angular range.

For verification of the HH polarized response, it was necessary to use a thicker cylinder since the contrast between the first- and second-order terms is insufficient with very thin cylinders. For cylinders with larger diameter to wavelength ratios than the one used for verification of the VV polarization case, NEC requires the use of a patch model. A patch model of a cylinder 18.0 cm in length and having a diameter of 0.55 cm was constructed using perfectly conducting patches. The model had 15 sides and consisted of over 800 rectangular patches. Because the patches were perfectly conducting, the axial standing wave made the model inappropriate for verification of the VV polarized case. However, the standing wave seems to have a much smaller effect as far as the HH response is concerned, becoming significant only for elevation angles less than about 30°. Figs. 9 and 10 present azimuth and elevation patterns for the cylinder/sphere pair having relative cylindrical coordinates $(\tilde{\rho}, \tilde{\phi}, \tilde{z}) = (2.0\text{ cm}, 45°, 9\text{ cm})$.

V. Conclusion

In this work a general technique based on the reciprocity theorem has been developed for deriving the secondary scat-

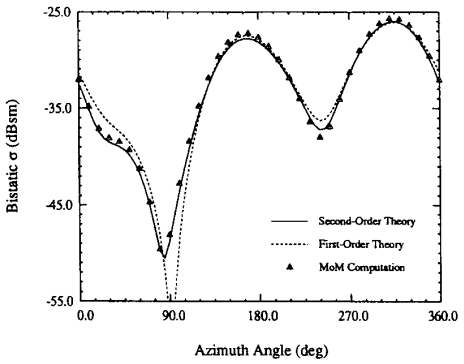

Fig. 9. Cylinder and sphere HH polarized scattering cross section at 9.25 GHz.

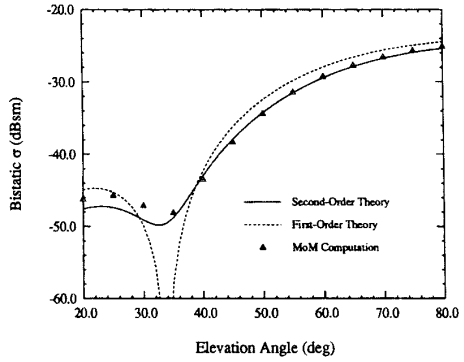

Fig. 10. Cylinder and sphere HH polarized scattering cross section at 9.25 GHz.

tered fields from a pair of objects. The general formulation has been applied to obtain approximate analytical expressions for the secondary scattered fields from a cylinder-sphere pair. The validity of the analytical results was verified by comparison with method of moments computations, and good agreement was obtained for both the co-polarized and cross-polarized bistatic scattering cross sections in the forward specular scattering cone. This work should provide the basis for the construction of computational simulations of electromagnetic wave scattering from heterogeneous two-component vegetation canopies that include the effects of multiple scattering up to second-order.

REFERENCES

[1] R. H. Lang and J. S. Sidhu, "Electromagnetic backscattering from a layer of vegetation: A discrete approach," *IEEE Trans. Geosci. Remote Sensing*, vol. 21, pp. 62–71, 1983.

[2] S. Seker, "Microwave backscattering from a layer of randomly oriented discs with application to scattering from vegetation," *IEE Proc., Microwave, Antennas and Propagation, H*, pp. 497–502, 1986.

[3] M. A. Karam, A. K. Fung, and Y. M. Antar, "Scattering models for vegetation samples," in *Proc. IEEE Geosci. Remote Sensing Symp.*, vol. 2, 1987, pp. 1013–1018.

[4] L. Tsang, M. C. Kubasci, and J. A. Kong, "Radiative transfer theory for active remote sensing of a layer of small ellipsoidal scatterers," *Radio Sci.*, vol. 16, pp. 321–329, 1981.

[5] M. C. Dobson, K. McDonald, and F. T. Ulaby, "Modeling of forest canopies and analysis of polarimetric SAR data," Univ. of Michigan Radiation Lab., Rep. 026143-1-F, 1988.

[6] M. W. Whitt and F. T. Ulaby, "Microwave scattering from periodic row-structured vegetation," Univ. of Michigan Radiation Lab., Rep. 026511-3-T, 1991.

[7] K. C. McDonald and F. T. Ulaby, "Modeling microwave backscatter from discontinuous tree canopies," Univ. of Michigan Radiation Lab., Rep. 026511-2-T, 1991.

[8] C. Liang and Y. T. Lo, "Scattering by two spheres," *Radio Sci.*, vol. 2, pp. 1481–1495, 1967.

[9] J. H. Bruning and Y. T. Lo, "Multiple scattering of EM waves by spheres, Part I—Multipole expansion and ray-optical solutions," *IEEE Trans. Antennas Propagat.*, vol. 18, pp. 378–390, 1971.

[10] K. Sarabandi, P. F. Polatin, and F. T. Ulaby, "Monte Carlo simulation of scattering from a layer of vertical cylinders," *IEEE Trans. Antennas Propagat.*, 1993, to be published.

[11] F. T. Ulaby, K. Sarabandi, K. McDonald, M. Whitt, and M. C. Dobson, "Michigan Microwave Canopy Scattering Model (MIMICS)," Univ. of Michigan Radiation Lab. Rep. 022486-3-T, 1988.

[12] ——, "Michigan microwave canopy scattering model," *Int. J. Remote Sensing*, vol. 11, pp. 1223–1253, 1990.

[13] M. A. Karam and A. K. Fung, "Scattering from randomly oriented circular discs with application to vegetation," *Radio Science*, vol. 18, pp. 557–565, 1983.

[14] ——, "Electromagnetic scattering from a layer of finite length, randomly oriented, dielectric circular cylinders over a rough interface with application to vegetation," *Int. J. Remote Sensing*, vol. 9, pp. 1109–1134, 1988.

[15] R. F. Harrington, *Time-Harmonic Electromagnetic Fields.* New York: McGraw-Hill, 1961.

[16] J. J. Bowman, T. B. A. Senior, and P. L. E. Uslenghi, *Electromagnetic and Acoustic Scattering by Simple Shapes.* New York: Hemisphere, 1987.

[17] H. C. Van de Hulst, *Light Scattering by Small Particles.* New York: Wiley, 1957.

[18] M. A. Karam and A. K. Fung, "EM scattering from a randomly oriented circular dielectric, finite-length cylinder," *International Union Radio Science Commission F: Wave Propagation and Remote Sensing, University of New Hampshire, Durham, New Hampshire*, 4.1.1–4.1.3.

[19] G. T. Ruck, D. E. Barrick, W. D. Stuart, and C. K. Krichbaum, *Radar Cross-Section Handbook.* New York: Plenum, 1970, pp. 273–274.

[20] T. B. A. Senior and K. Sarabandi, *Radar Polarimetry for Geoscience Applications*, F. T. Ulaby, and C. Elachi, Eds. Norwood, MA: Artech House, 1990, p. 95.

[21] G. J. Burke and A. J. Poggio, *Numerical Electromagnetics Code (NEC)—Method of Moments*, Lawrence Livermore National Laboratory, 1981.

[22] ——, *Numerical Electromagnetics Code (NEC)—Method of Moments*, Naval Ocean Systems Center, Technical Document 116, Vol. 2, 1981.

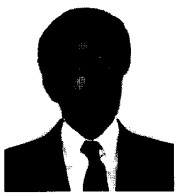

Kamal Sarabandi (S'87–M'90–SM'93) received the B.S. degree in electrical engineering from Sharif University of Technology, Tehran, Iran, in 1980. From 1980 to 1984 he worked as a microwave engineer in the Telecommunication Research Center in Iran. He entered the graduate program at the University of Michigan in 1984 and received the M.S.E. degree in electrical engineering in 1986, and the M.S. degree in mathematics and the Ph.D. degree in electrical engineering in 1989.

He is presently an assistant professor in the Department of Electrical Engineering and Computer Science at the University of Michigan. His research interests include electromagnetic scattering, microwave and millimeter wave remote sensing, computational electromagnetics, and calibration of polarimetric SAR systems.

Dr. Sarabandi is the elected chairman of Geoscience and remote sensing Michigan chapter and a member of the Electromagnetics Academy and USNC/URSI Commission F.

Paul F. Polatin was born in New York City on March 18, 1956. He received the B.A. and M.A. degrees in chemical physics from Columbia University in 1978 and 1979, respectively.

From 1978 to 1983 he was involved in various research projects including nuclear quadrupole resonance spectroscopy and near-infrared reflectance spectroscopy. From 1984 to 1987 he was with the Upjohn Pharmaceutical Company as a research chemist and laboratory supervisor. In 1987 he joined the Radiation Laboratory at the University of Michigan where he received the M.S. (1989) and Ph.D. (1993) degrees, both in electrical engineering. His research work at the Radiation Laboratory was concerned with the scattering of electromagnetic waves by random media and other problems related to remote sensing of the terrestrial environment. At present he is employed by the MITRE Corporation of Bedford, MA, in the Advanced Satellite Terminals Division.